Journal of Porous Media, 3(2), 155–164 (2000)

Simultaneous Heat and Mass Transfer by Natural Convection from a Cone and a Wedge in Porous Media

Ali J. Chamkha, Abdul-Rahim A. Khaled, and Osamah al-Hawaj

Department of Mechanical and Industrial Engineering, Kuwait University, P.O. Box 5969, Safat, 13060 Kuwait

ABSTRACT

The problem of steady, laminar, hydromagnetic simultaneous heat and mass transfer by natural convection flow over a vertical cone and a wedge embedded in a uniform porous medium is investigated. Two cases of thermal boundary conditions, namely the uniform wall temperature (UWT) and the uniform wall heat flux (UHF), are considered. A nonsimilarity transformation for each case is employed to transform the governing differential equations to a form whereby they produce their own initial conditions. The transformed equations for each case are solved numerically by an efficient implicit, iterative, finite-difference scheme. The obtained results are checked against previously published work on special cases of the problem and are found to be in excellent agreement. A parametric study illustrating the influence of the magnetic field, porous medium inertia effects; heat generation or absorption; lateral wall mass flux; concentration to thermal buoyancy ratio; and the Lewis number on the fluid velocity, temperature, and concentration as well as the Nusselt and the Sherwood numbers is conducted. The results of this parametric study are shown graphically and the physical aspects of the problem are discussed. It is concluded that while the local Nusselt number decreases owing to the imposition of the magnetic field, it increases as a result of the fluid's absorption effects. Also, both the local Nusselt and Sherwood numbers increase as the buoyancy ratio increases. This is true for both uniform wall temperature and heat flux thermal conditions. Furthermore, including the porous medium inertia effect in the mathematical model is predicted to decrease the local Nusselt number for both the isothermal and isoflux wall cases.

Received July 30, 1998; Accepted December 1, 1998

NOMENCLATURE

B_o	magnetic field strength
C	concentration at any point in the field
C_o	reference concentration at the wall for UHF
C_∞	concentration at the free stream
C_w	concentration at the wall
c_p	specific heat of the ambient fluid
D	mass diffusivity
e	buoyancy ratio
F	inertia coefficient of the porous medium
f, f^*	dimensionless stream function
g	gravitational acceleration
h	local convective heat transfer coefficient
h_m	local mass transfer coefficient
K	permeability of the porous medium
k_e	effective thermal conductivity of the porous medium
L	characteristic length of the plate
Le	Lewis number
M	square of the Hartmann number
Nu	local Nusselt number
n	geometric factor
Pr	Prandtl number
Q_o	internal heat generation or absorption coefficient
q_w	heat flux at the wall for UHF
Ra_x	local Rayleigh number for UWT
Ra_x^*	local Rayleigh number for UHF
Ra_L	Rayleigh number based on the characteristic length for UWT
Ra_L^*	Rayleigh number based on the characteristic length for UHF
Sh	local Sherwood number
T	temperature at any point
T_w	wall temperature for UWT
u	tangential velocity
UHF	uniform wall heat flux
UWT	uniform wall temperature
v	normal velocity
V_w	wall mass flux coefficent
x	distance along the cone or the wedge
y	distance normal to the cone or the wedge

Greek symbols

Γ	dimensionless porous medium inertia coefficient
α_e	effective thermal diffusivity of the porous medium
β_C	concentration expansion coefficient
β_T	thermal expansion coefficient
δ	dimensionless internal heat generation or absorption parameter
ε	porosity of the porous medium
ϕ, ϕ^*	transformed concentration
γ	half angle of the cone or the wedge
η, η^*	coordinate transformation in terms of x and y
μ	fluid dynamic viscosity
υ	fluid kinematic viscosity
ψ	stream function
θ, θ^*	transformed temperature
ρ	fluid density
σ	fluid electrical conductivity
ξ, ξ^*	coordinate transformation for x

INTRODUCTION

Simultaneous heat and mass transfer from different geometries embedded in porous media has many engineering and geophysical applications such as geothermal reservoirs, drying of porous solids, thermal insulation, enhanced oil recovery, packed-bed catalytic reactors, cooling of nuclear reactors, and underground energy transport. Most early studies on porous media have used the Darcy law, which is a linear empirical relationship between the Darcian velocity and the pressure drop across the porous medium and is limited to slow flows. However, for high velocity flow situations, the Darcy law is inapplicable because it does not account for the resulting inertia effects of the porous medium. In this situation, the relationship between the velocity and the pressure drop is quadratic. The high flow situation is established when the Reynolds number based on the pore size is greater than unity. Vafai and Tien (1981) have discussed the importance of inertia effects for flows in porous media.

Cheng and Minkowycz (1977) have used the Darcy law in their study on free convection about a vertical impermeable flat plate in porous media. The problem of a vertical cylinder embedded in porous media has been investigated by Minkowycz and Cheng (1976) using the local nonsimilarity method and by Kumari et al. (1985) using the finite difference and improved perturbation methods. Cheng et al. (1985) have analyzed the problem of natural convection of a Darcian flow about a cone using the local nonsimilarity method. More recently, Lai (1991) has investigated coupled heat and mass transfer by mixed convection from an isothermal vertical plate in a porous medium. Yih (1997) has studied the effect of transpiration on the problem of Lai (1991). The case of variable wall temperature and concentration in the presence of a magnetic field force has been considered by Elbashbeshy (1997). Chamkha (1996) has obtained similarity solutions for the problem of non-Darcy free convection from a nonisothermal cone and a wedge in a porous medium. Yih (1997) have reported on the effect of uniform lateral mass flux on free convection about a vertical cone embedded in a fluid-saturated porous medium.

There has been a renewed interest in studying magnetohydrodynamic (MHD) flow and heat transfer in porous and nonporous media as a result of the effect of magnetic fields on the performance of many systems using electrically conducting fluids. For example, Raptis et al. (1982) have analyzed hydromagnetic free convection flow through a porous medium between two parallel plates. Kafoussias (1992) has considered MHD free convection flow through a nonhomogeneous porous medium over an isothermal cone surface. Aldoss et al. (1995) have studied mixed convection from a vertical plate embedded in a porous medium in the presence of a magnetic field. Bian et al. (1995) have reported on the effect of an electromagnetic field on natural convection in an inclined porous medium. Buoyancy-driven convection in a rectangular enclosure with a transverse magnetic field has been considered by Garandet et al. (1992).

In certain porous media applications such as those involving heat removal from nuclear fuel debris, underground disposal of radioactive waste material, storage of food stuffs, and exothermic chemical reactions in packed-bed reactors, the working fluid heat generation (source) or absorption (sink) effects are important. Representative studies dealing with these effects have been reported by such authors as Acharya and Goldstein (1985), Vajravelu and Nayfeh (1992), and Chamkha (1996, 1997).

The objective of this article is to consider simultaneous heat and mass transfer by natural convection about a vertical wedge and a cone embedded in a fluid-saturated porous medium in the presence of lateral mass flux, magnetic field effects, heat generation or absorption effects, and porous medium inertia effects. This is done for both uniform wall temperature (UWT) and uniform wall heat flux (UHF) situations.

PROBLEM DEFINITION

Consider steady, laminar, hydromagnetic coupled heat and mass transfer by natural convection flow over a stationary cone embedded in a fluid-saturated porous medium. Figure 1 shows the schematic diagram of the problem. The origin of the coordinate system is placed at the vertex of the cone, where the x-direction is taken along the cone and the y-direction is normal to the cone. A magnetic field of uniform strength B_0 is applied in the y-direction that is normal to the surface of the cone. The fluid is assumed to be Newtonian, electrically conducting, heat generating or absorbing, and has constant properties except the density in the buoyancy term of the balance of momentum equation. Also, the porosity and the permeability of the porous medium are assumed to be constant. The fluid and the porous medium are assumed to be in local thermal equilibrium. The surface of the cone is kept at either constant wall temperature or heat flux and constant or variable concentration. The temperature and the concentration at the cone surface are always greater than their uniform ambient values existing far from the cone surface. The magnetic Reynolds number is assumed to be small so that the induced magnetic field can be neglected. In addition, there

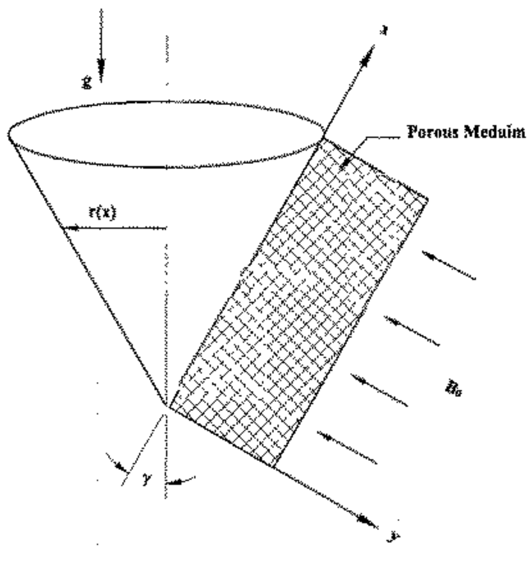

Figure 1. Flow model and coordinate system.

is no applied electric field and the Hall effect, Joule heating, and viscous dissipation are all neglected in this work. It is worth noting that generating a magnetic field around a cone may require the physical cone to be embedded coaxially in a magnetized conical shell.

The governing equations that take into account the inertia effect of the porous medium within the boundary layer and Boussinseq approximations may be written as follows:

$$\frac{\partial(r^n u)}{\partial x}+\frac{\partial(r^n v)}{\partial y}=0 \tag{1}$$

$$\left(1+\frac{\sigma B_0^2 K}{\rho\upsilon\varepsilon}+\frac{2FK}{\rho\upsilon}u\right)\frac{\partial u}{\partial y}=\frac{g\beta_T K\cos\gamma}{\upsilon}\frac{\partial T}{\partial y}+\frac{g\beta_C K\cos\gamma}{\upsilon}\frac{\partial C}{\partial y} \tag{2}$$

$$u\frac{\partial T}{\partial x}+v\frac{\partial T}{\partial y}=\alpha_e\frac{\partial^2 T}{\partial y^2}+\frac{Q_0}{\rho c_p}(T-T_\infty) \tag{3}$$

$$u\frac{\partial C}{\partial x}+v\frac{\partial C}{\partial y}=D\frac{\partial^2 C}{\partial y^2} \tag{4}$$

The boundary conditions are defined as follows:

$$y=0:\quad v=V_w,\quad T=T_w,\quad C=C_w \tag{5}$$

$$y\to\infty:\quad u=0,\quad T=T_\infty,\quad C=C_\infty \tag{6}$$

If a uniform heat flux q_w is prescribed at the boundary, Eqs. (5) are replaced by

$$y=0:\quad v=V_w,\quad -k_e\left(\frac{\partial T}{\partial y}\right)_{y=0}=q_w,\quad C=C_w \tag{7}$$

where u, v, T, and C are the fluid x-component of velocity, y-component of velocity, temperature, and concentration, respectively. u and v become the Darcian velocities when F is set to zero. ρ, υ, c_p, β_T, and β_c are the fluid density, kinematic viscosity, specific heat at constant pressure, coefficient of thermal expansion, and coefficient of concentration expansion, respectively. σ, Q_0, and D are the fluid electrical conductivity, heat generation (>0) or absorption (<0) coefficient, and mass diffusivity, respectively. g and B_o are the gravitational acceleration and magnetic induction, respectively. ε, K, F, k_e, and α_e are the porous medium porosity, permeability, inertia coefficient, effective thermal conductivity of the saturated porous medium and the effective thermal diffusivity, respectively. T_∞ and C_∞ are the ambient fluid temperature and concentration, respectively. V_w (a constant) is the surface mass flux coefficient. T_w, C_w, and γ are the wall temperature and concentration and the cone half angle, respectively. The value of n can be either $n=0$ for flow over a vertical wedge or $n=1$ for flow over a vertical cone. When $n=0$ and $\gamma=0$, the problem will reduce to the case of a vertical flat plate as mentioned by Yih (1997). The above equations were derived under the assumption that the boundary-layer thickness is sufficiently thin relative to the local radius of the cone. Thus, the local radius to a point in the boundary layer can be replaced by the radius of the cone ($x=r\sin\gamma$). It is worth noting that the mathematical model used in this article is based on a modified Darcy law to include inertia effects. Other more enhanced models (Vafai and Tien, 1981) have also included the boundary effects in Eq. (2). This is not done here.

Uniform Wall Temperature (UWT)

Invoking the following dimensionless variables that were reported earlier by Yih (1997):

$$\xi=\frac{2V_w}{\alpha_e Ra_x^{1/2}}x \tag{8}$$

$$\eta=\frac{y}{x}Ra_x^{1/2} \tag{9}$$

$$f(\xi,\eta)=\frac{\psi}{\alpha_e r^n Ra_x^{1/2}} \tag{10}$$

$$\theta(\xi,\eta)=\frac{T-T_\infty}{T_w-T_\infty} \tag{11}$$

$$\phi(\xi,\eta)=\frac{C-C_\infty}{C_w-C_\infty} \tag{12}$$

where $Ra_x=g\cos\gamma\beta_T K(T_w-T_\infty)x/(\upsilon\alpha_e)$ is the local Rayleigh number for the case of UWT yields

$$(1+M+\Gamma f')f''=\theta'+e\phi' \tag{13}$$

$$\theta''+\left(n+\frac{1}{2}\right)f\theta'+\delta\xi^2\theta=\frac{1}{2}\xi\left(f'\frac{\partial\theta}{\partial\xi}-\theta'\frac{\partial f}{\partial\xi}\right) \tag{14}$$

$$\frac{1}{Le}\phi''+\left(n+\frac{1}{2}\right)f\phi'=\frac{1}{2}\xi\left(f'\frac{\partial\phi}{\partial\xi}-\phi'\frac{\partial f}{\partial\xi}\right) \tag{15}$$

where

$$M=\frac{\sigma B_0^2 K}{\rho\upsilon\varepsilon},\qquad \Gamma=\frac{2FK\alpha_e Ra_L}{\rho\upsilon L},\qquad e=\frac{\beta_C(C_w-C_\infty)}{\beta_T(T_w-T_\infty)} \tag{16}$$

$$Le = \frac{\alpha_e}{D}, \qquad \delta = \frac{Q_o}{4k_e}\left(\frac{\alpha_e}{V_W}\right)^2, \qquad Ra_L = \frac{g\beta_T K \cos\gamma (T_W - T_\infty)L}{\upsilon \alpha_e} \tag{17}$$

are the square of the Hartmann number, dimensionless porous medium inertia coefficient, buoyancy ratio, Lewis number, dimensionless internal heat generation or absorption parameter, and the Rayleigh number at $x = L$ where L is a characteristic length along the x-direction.

The boundary conditions after transformation will be

$$\eta = 0 \qquad f = -\frac{\xi}{2n+2}, \quad \phi = 1, \quad \phi = 1 \tag{18}$$

$$\eta \to \infty; \qquad f' = 0, \quad \theta = 0, \quad \phi = 0 \tag{19}$$

Uniform Wall Heat Flux (UHF)

For the case of uniform wall heat flux, the following dimensionless variables has also been suggested by Yih (1997):

$$\xi^* = \frac{2V_w}{\alpha_e Ra_x^{*1/3}} x \tag{20}$$

$$\eta^* = \frac{y}{x} Ra_x^{*1/3} \tag{21}$$

$$f^*(\xi^*, \eta^*) = \frac{\psi}{\alpha_e r^n Ra_x^{*1/3}} \tag{22}$$

$$\theta^*(\xi^*, \eta^*) = \frac{(T - T_\infty)k_e Ra_x^{*1/3}}{q_w x} \tag{23}$$

$$\theta^*(\xi^*, \eta^*) = \frac{C - C_\infty}{C_w - C_\infty} \tag{24}$$

where $Ra_x^* = g \cos\gamma\beta_T K q_w x^2/(\upsilon\alpha_e k_e)$ is the local Rayleigh number for the case of UHF. As a result of substituting Eqs. (20)–(24) into Eqs. (1)–(4), the following nonsimilar equations will be obtained.

$$\left(1 + M + \Gamma\xi^* f^{*'}\right) f^{*''} = \theta^{*'} + e\phi^{*'} \tag{25}$$

$$\theta^{*''} + \left(n + \frac{2}{3}\right) f^* \theta^{*'} - \frac{1}{3} f^* \theta^{*'} + \delta\xi^{*2}\theta^* = \frac{1}{2}\xi^*\left(f^{*'}\frac{\partial\theta^*}{\partial\xi^*} - \theta^{*'}\frac{\partial f^*}{\partial\xi^*}\right) \tag{26}$$

$$\frac{1}{Le}\phi^{*''} + \left(n + \frac{2}{3}\right) f^* \phi^{*'} - \frac{1}{3} f^* \phi^{*'} = \frac{1}{2}\xi^*\left(f^{*'}\frac{\partial\phi^*}{\partial\xi} - \phi^{*'}\frac{\partial f^*}{\partial\xi^*}\right) \tag{27}$$

where

$$M = \frac{\sigma B_o^2 K}{\rho\upsilon\varepsilon}, \qquad \Gamma = \frac{F\alpha_e^2 K Ra_L^*}{\rho\upsilon L^2 V_w} \tag{28}$$

$$Le = \frac{\alpha_e}{D}, \qquad \delta = \frac{Q_o}{4k_e}\left(\frac{\alpha_e}{V_w}\right)^2, \qquad Ra_L^* = \frac{g\beta_T \cos\gamma K q_w L^2}{\upsilon\alpha_e k_e} \tag{29}$$

are the square of the Hartmann number, dimensionless porous medium inertia coefficient, buoyancy ratio, Lewis number, dimensionless internal heat generation or absorption parameter, and the Rayleigh number at $x = L$ for the UHF case.

The boundary conditions for this case transform to

$$\eta^* = 0: \qquad f^* = -\frac{\xi^*}{2n+2}, \quad \theta^{*'} = -1, \quad \phi^* = 1 \tag{30}$$

$$\eta^* \to \infty: \qquad f^{*'} = 0, \quad \theta^* = 0, \quad \phi^* = 0 \tag{31}$$

where the condition for a constant buoyancy ratio $e(e = g \cos\gamma\beta_C K(C_w - C_\infty)x/(\upsilon Ra_x^{*2/3})$ requires that the wall fluid concentration varies according to

$$\frac{C_w - C_\infty}{C_0 - C_\infty} = \left(\frac{x}{L}\right)^{1/3} \tag{32}$$

The local Nusselt number and the local Sherwood number for constant wall temperature condition for both wedge and cone can be computed from the following relationships:

$$Nu = \frac{hx}{k_e} = -\theta'(\xi, 0) Ra_x^{1/2} \tag{33}$$

$$Sh = \frac{h_m x}{D} = -\phi'(\xi, 0) Ra_x^{1/2} \tag{34}$$

and the corresponding numbers for uniform wall heat flux will be

$$Nu = \frac{hx}{k_e} = \frac{1}{\theta^*(\xi^*, 0)} Ra_x^{*1/3} \tag{35}$$

$$Sh = \frac{h_m x}{D} = -\phi^{*\prime}(\xi^*, 0) Ra_x^{*1/3} \tag{36}$$

where h and h_m are the local convective heat transfer coefficient and the local mass diffusion coefficient, respectively.

NUMERICAL METHOD

The nonsimilar equations for the cases of uniform wall temperature or heat flux have been linearized and then descritized using three-point central difference quotients with variable step sizes in the η or η^* directions and using two-point backward difference formulae in the ξ or ξ^* directions with constant step sizes. The resulting equations form a tridiagonal system of algebraic equations that can be solved by the well-known Thomas algorithm (see Blottner, 1970). The solution process starts at $\xi = 0$ or $\xi^* = 0$ and then proceeds forward using the solution at the previous line of constant ξ or ξ^* to $\xi = 1$ or $\xi^* = 1$. Because of the nonlinearities of the equations, an iterative solution with successive over- or underrelaxation techniques is required. The maximum absolute error between two successive iterations was taken to be 10^{-6} for convergence. A starting step size of 0.001 in the η or η^* direction with an increase of 1.03 times the previous step size and a constant step size in the ξ or ξ^* direction of 0.1 were found to give accurate results. The maximum value of η or η^* that represents the ambient conditions was assumed to be 50. The accuracy of the aforementioned numerical method was validated by direct comparisons with the numerical results reported earlier by Yih (1997) for the cases of a vertical plate ($n = 0$, $\gamma = 0$) and a cone ($n = 1$) in the absence of magnetic, heat generation or absorption, and concentration buoyancy effects. Tables 1 and 2 present the results of these comparisons. It can be seen from these tables that excellent agreement between the results exists. These favorable comparisons lend confidence in the numerical results to be reported in the next section.

RESULTS AND DISCUSSION

Table 3 gives the parametric conditions for each of the curves shown in Figs. 2–9.

Figures 2 and 3 represent the behavior of the stream function and the fluid velocity for the situations shown in Table 3 for both a cone and a wedge at positive lateral wall mass flux for uniform wall temperature at $\xi = 10$. The presence of a magnetic field in an electrically conducting fluid tends to produce a body force against the flow. This type of resistive force tends to slow down the flow which, in turn, reduces the stream function as shown in curve II compared to the reference curve I in both figures. An additional resistance against the flow exists if the porous medium inertia effect is considered especially at high velocities. As a result, the flow stream function and velocities near the wall decrease as depicted from curves III and III* compared with curves I and II for a cone and a wedge, respectively. Curve IV shows the effect of internal heat absorption on both the stream function and the velocity. The value of $\delta = -1$ represents a large value of a heat sink that causes the temperature of the fluid to reduce to the free stream temperature at rapid rates, as shown in curve IV in Figure 4, which, in turn, eliminates the thermal buoyancy forces. Accordingly, the hydrodynamic boundary-layer thickness will be very small and the stream function will be almost constant. Including mass diffusion results in an increase in the flow velocities and stream function due to

Table I

Values for $-\theta'(\xi, 0)$ for the Cases of Wedge ($n = 0$) and Cone ($n = 1$) at UWT ($e = 0$, $M = 0$, $\delta = 0$, $\Gamma = 0$)

ξ	$n = 0$ Yih (1997)	$n = 0$ Present Method	$n = 1$ Yih (1997)	$n = 1$ Present Method
−10	4.9999	4.9830	5.0995	5.0857
−8	3.9999	3.9892	4.1244	4.1156
−6	2.9999	2.9936	3.1655	3.1603
−4	2.0015	1.9976	2.2434	2.2409
−2	1.0725	1.0722	1.4139	1.4132
0	0.4437	0.4439	0.7686	0.7686
2	0.1416	0.1423	0.3537	0.3541
4	0.0333	0.0340	0.1342	0.1349
6	0.0055	0.0058	0.0400	0.0411
8	0.0006	0.0007	0.0092	0.0096
10	0.0001	0.0001	0.0016	0.0017

Table 2

Values for $\theta^*(\xi^*, 0)$ for the Cases of Wedge ($n = 0$) and Cone ($n = 1$) at UHF ($e = 0$, $M = 0$, $\delta = 0$, $\Gamma = 0$)

ξ^*	n = 0 Yih (1997)	$n = 0$ Present Method	$n = 1$ Yih (1997)	$n = 1$ Present Method
−10	0.2000	0.2004	0.1992	0.1996
−8	0.2500	0.2504	0.2480	0.2484
−6	0.3333	0.3338	0.3272	0.3276
−4	0.4993	0.5005	0.4695	0.4701
−2	0.8473	0.8478	0.7198	0.7200
0	1.2962	1.2964	1.0564	1.0566
2	1.7398	1.7393	1.4272	1.4268
4	2.1524	2.1510	1.8041	1.8032
6	2.5296	2.5277	2.1748	2.1718
8	2.8740	2.8720	2.5304	2.5256
10	3.1901	3.1880	2.8663	2.8612

Table 3

Parametric Values for Curves in the Figures

Curve	E	Le	M	Γ	δ
I	0	0	0	0	0
II	0	0	1.0	0	0
III*	0	0	1.0	0.5	0
III	0	0	0	0.1	0
IV	0	0	0	0	−1.0
V	0.5	0.5	0	0	0
VI	0.5	1.25	0	0	0

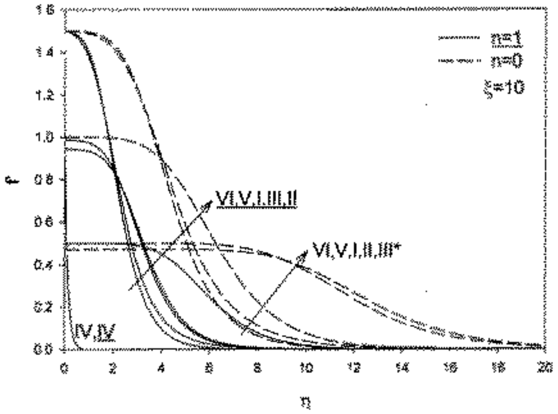

Figure 3. Variations of tangential velocity with e, Le, M, Γ, δ for UWT.

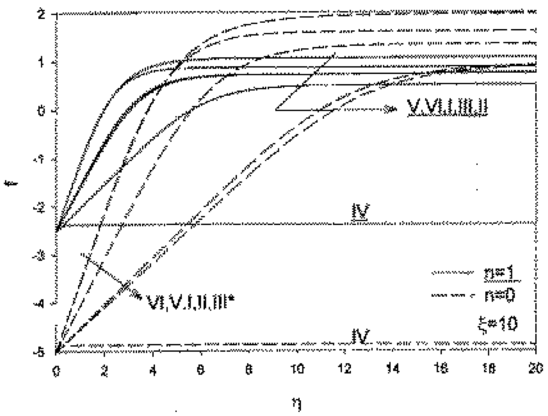

Figure 2. Variations of stream function with e, Le, M, Γ, and δ for UWT.

additional concentration buoyancy forces. This is shown by curve V and VI for different Lewis numbers compared to curve I where the concentration buoyancy forces are excluded.

Figures 4 and 5 illustrate the temperature and the velocity profiles for a cone and a wedge at uniform wall temperature under the presence of positive lateral wall mass flux at $\xi = 10$. The resistive force discussed in the previous paragraph due to the presence of a magnetic field in an electrically conducting fluid increases the temperatures in the flow and, as a result, reduces the heat transfer from the wall. This fact is shown by curve II compared to curve

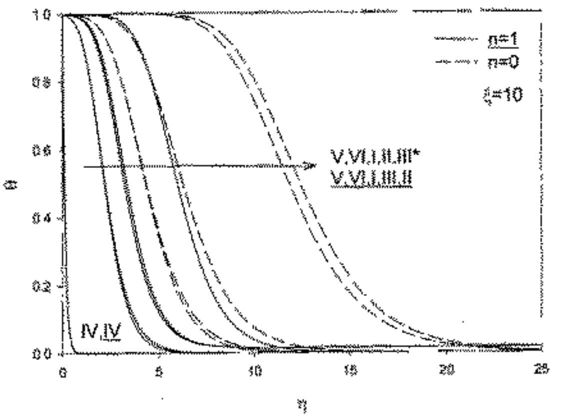

Figure 4. Variations of temperature with e, Le, M, Γ, and δ and UWT.

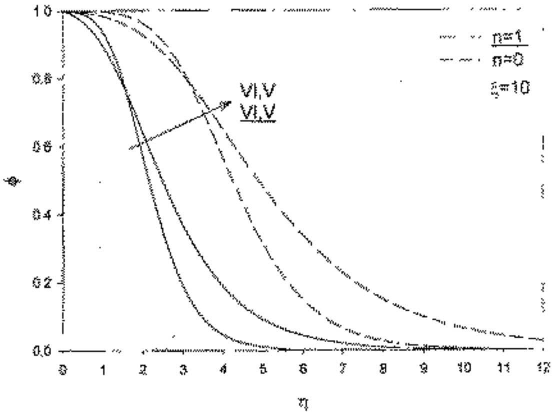

Figure 5. Variations of concentration with e and Le for UWT.

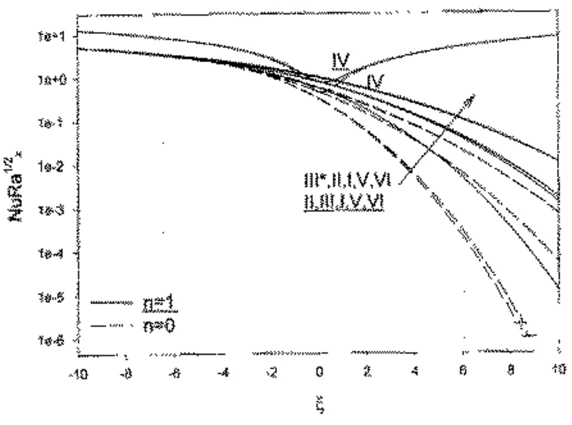

Figure 6. Variations of Nusselt number with e, Le, M, Γ, and δ for UWT.

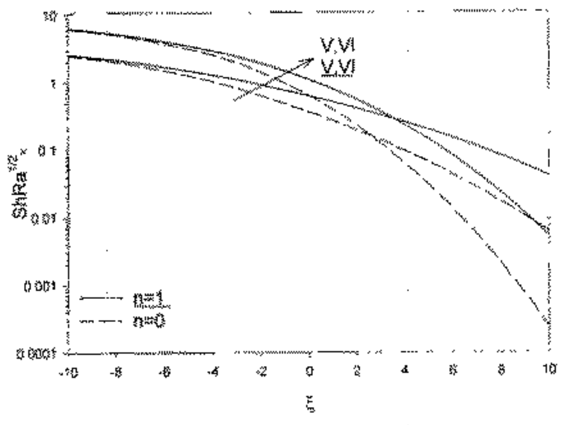

Figure 7. Variations of Sherwood number with e and Le for UWT.

I where the wall temperature slope is very small. The porous medium inertia effect tends to increase the temperature of the flow due to the effect of a decrease in the momentum diffusion as discussed before and observed in curves III and III* compared to curves I and II for a cone and a wedge, respectively. Furthermore, the additional concentration buoyancy forces, found in curves V and VI, decrease the temperature of the flow due to the increase in the flow velocity. The concentration boundary-layer thickness decreases at higher Lewis numbers but the absolute wall concentration slopes are higher for lower Lewis numbers as shown in curves V and VI in Fig. 5. These are due to the effect of lateral blowing wall mass flux.

Figures 6 and 7 illustrate the distribution of the local Nusselt and Sherwood numbers for a cone and a wedge at uniform wall temperature under the presence of equal positive or negative lateral wall mass fluxes. Due to the increases in the flow temperatures and decrease in the absolute wall temperature slopes when the magnetic field is present, the local Nusselt number reduces. This fact is illustrated by curve II compared to curve I. Also, the porous medium inertia effect tends to decrease the local Nusselt number due to its effect on the wall temperature slopes as

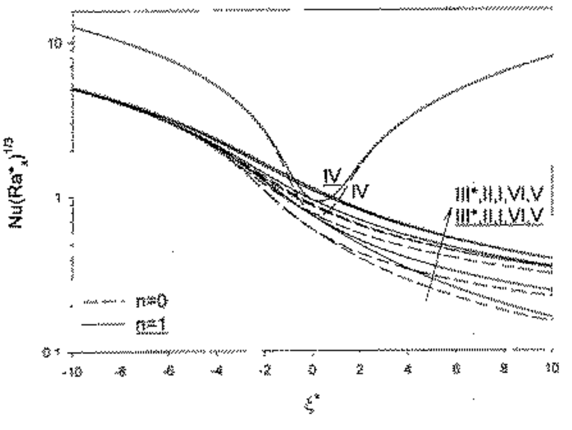

Figure 8. Variations of Nusselt number with ϵ, Le, M, Γ, and δ for UHF.

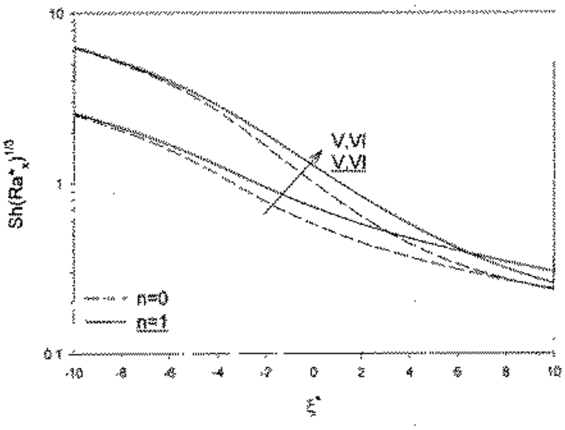

Figure 9. Variations of Sherwood number with ϵ and Le for UHF.

one can see from curves III and III* compared to curves I and II for a cone and a wedge, respectively. Although the local Nusselt number is higher when the fluid has internal heat absorption (curve IV) compared to the reference case I, the effect of lateral mass injection flux from the wall is the same for equal lateral mass suction flux from the wall. Furthermore, curves V and VI confirm the fact that including the mass diffusion equation increases the local Nusselt number. For all of the above cases the local Nusselt number is the same at large wall mass suction flux and large x, as observed from Fig. 6, as the hydrodynamic and the thermal boundary-layer thicknesses will be very small. Curves V and VI in Fig. 7 show that the local Sherwood number for $Le = 1.25$ is higher than that for $Le = 0.5$ up to a certain point where the lateral mass wall blowing tends to decrease the local Sherwood number.

For the case of uniform wall heat flux, similar effects on the velocity and temperature profiles as the case of uniform wall temperature are obtained by varying the parameters in Table 3. Compared with the reference case in Table 3, the flow velocities near the wall and the reciprocal of the wall temperature are lower for the cases where a magnetic field is present and the porous medium inertia effect is considered while they are higher when the fluid absorbs thermal energy for reasons similar to those for the UWT condition. Because the local Nusselt number is inversely proportional to the wall temperature, the values of the local Nusselt number will be reduced except for the case of internal heat absorption in which they increase as shown in Fig. 8. Also, the trend of the local Nusselt and Sherwood numbers when the buoyancy ratio is included and the Lewis number is changed are shown in Figs. 8 and 9, respectively.

CONCLUSION

The problem of steady, laminar, simultaneous heat and mass transfer by natural convection boundary-layer flow of an electrically conducting and heat generating or absorbing fluid over an isothermal or isoflux vertical and permeable with constant lateral wall mass flux cone or wedge embedded in a uniform porous medium was considered. The governing equations for both situations of uniform wall temperature (UWT) and uniform wall heat flux (UHF) were developed and transformed using appropriate nonsimilarity transformations. The transformed equations were then solved numerically by an implicit, iterative, finite-difference scheme. The obtained results for special cases of the problem were compared with previously published work and were found to be in excellent agreement. It was found that while the Nusselt number decreased as a result of the presence of either the magnetic field or positive lateral wall mass flux, they increased as a result of imposition of negative lateral wall mass flux for both the uniform wall temperature and the uniform wall heat flux cases. Also, the Nusselt number was increased because of the presence of heat absorption effects for both cases. In addition, the Nusselt number decreased when considering the porous medium inertia effect for both the uniform wall temperature and heat flux cases. Furthermore, increasing the ratio of concentration to thermal buoyancies was found to cause enhancements in the values of the Nusselt number and the Sherwood number for the two studied thermal cases. It is hoped that the present work will serve as a vehicle for understanding more complex problems involving the various physical effects investigated in the present problem.

REFERENCES

Acharya, S. and Goldstein, R.J., Natural convection in an externally heated vertical or inclined square box containing internal energy sources, *ASME J. Heat Transfer,* vol. 107, pp. 855–866, 1985.

Aldoss, T.K., Al-Nimr, M.A., Jarrah, M.A. and Al-Sha'er, B.J., Magnetohydrodynamic mixed convection from a vertical plate embedded in a porous medium, *Numer. Heat Transfer,* vol. 28A, pp. 635–645, 1995.

Bian, W., Vasseur, P., and Meng, F., Effect of electromagnetic field on natural convection in an inclined porous medium, *Int. J. Heat Fluid Flow,* vol. 17, pp. 36–44, 1996.

Blottner, F.G., Finite-difference methods of solution of the boundary-layer equations, *AIAA J.,* vol. 8, pp. 193–205, 1970.

Chamkha, A.J., Non-Darcy hydromagnetic free convection from a cone and a wedge in porous media, *Int. Commun. Heat Mass Transfer,* vol. 23, pp. 875–887, 1996.

Chamkha, A.J., Non-Darcy fully developed mixed convection in a porous medium channel with heat generation/absorption and hydromagnetic effects, *Numer. Heat Transfer,* vol. 32, pp. 853–875, 1997.

Cheng, P. and Minkowycz, W.J., Free convection about a vertical flat plate embedded in a porous medium with application to heat transfer from a dike, *J. Geophys.,* vol. 82, pp. 2040–2044, 1977.

Cheng, P., Le, T., and Pop, I., Natural convection of a Darcian fluid about a cone, *Int. Commun. Heat Mass Transfer,* vol. 12, pp. 705–717, 1985.

Elbashbeshy, E.M.A., Heat and mass transfer along a vertical plate with variable surface tension and concentration in the presence of the magnetic field, *Int. J. Eng. Sci.,* vol. 34, pp. 515–522, 1997.

Garandet, J.P., Alboussiere, T., and Moreau, R., Driven convection in a rectangular enclosure with a transverse magnetic field, *Int. J. Heat Mass Transfer,* vol. 34, pp. 741–748, 1992.

Kafoussias, N.G., MHD free convection flow through a nonhomogeneous porous medium over an isothermal cone surface, *Mech. Res. Commun,* vol. 19, pp. 89–94, 1992.

Kumari, M., Pop, I., and Nath, G., Finite difference and improved perturbation solutions for free convection on a vertical cylinder embedded in a saturated porous medium, *Int. J. Heat Mass Transfer,* vol. 28, pp. 2171–2174, 1985.

Lai, F.C., Coupled heat and mass transfer by mixed convection from a vertical plate in a saturated porous medium, *Int. Commun. Heat Mass Transfer,* vol. 18, pp. 93–106, 1991.

Minkowycz, W.J. and Cheng, P., Free convection about a vertical cylinder embedded in a porous medium, *Int. J. Heat Mass Transfer,* vol. 19, pp. 805–513, 1976.

Raptis, A., Massias, C., and Tzivanidis, G., Hydromagnetic free convection flow through a porous medium between two parallel plates, *Phys. Lett,* vol. 90A, pp. 288–289, 1982a.

Vafai, K. and Tien, C.L., Boundary and inertia effects on flow and heat transfer in porous media, *Int. J. Heat Mass Transfer,* vol. 24, pp. 195–203, 1981.

Vajravelu, K. and Nayfeh, J., Hydromagnetic convection at a cone and a wedge, *Int. Commun. Heat Mass Transfer,* vol. 19, pp. 701–710, 1992.

Yih, K.A., The effect of transpiration on coupled heat and mass transfer in mixed convection over a vertical plate embedded in a saturated porous medium, *Int. Commun. Heat Mass Transfer,* vol. 24, pp. 265–275, 1997.

Yih, K.A., The effect of uniform lateral mass flux on free convection about a vertical cone embedded in a saturated porous medium, *Int. Commun. Heat Mass Transfer,* vol. 24, pp. 1195–1205, 1997.